A Method for Derivation of Robot Task-Frame Control Authority from Repeated Sensory Observations

Luka Peternel*, Leonel Rozo, Darwin Caldwell and Arash Ajoudani

***Abstract*—In this paper we propose a novel method that enables the robot to autonomously devise an appropriate control strategy from human demonstrations without a prior knowledge of the demonstrated task. The method is primarily based on observing the patterns and consistency in the observed dataset. This is obtained through a demonstration setting that uses a motion capture system, a force sensor and muscle activity measurements. The variables (position and force) in the collected dataset are then segmented and analysed for each axis of the observed task frame separately. While checking several conditions based on the consistency, value range, and magnitude of repeated observations, the appropriate controller (i.e. position or force) is delegated to each axis of the task frame. In the final stage, the method also checks for correlation between variables and muscle activity patterns to determine the desired stiffness behaviour. The robot then uses the derived control strategies in autonomous operation through a hybrid force/impedance controller. To validate the proposed method we performed experiments on real-life tasks involving physical interaction with the environment, where we considered surface wiping, material sawing and drilling.**

***Index Terms*—Learning and Adaptive Systems, Motion Control of Manipulators, Force Control, Compliance and Impedance Control**

I. Introduction

CURRENTLY one of the primary focuses of robotics is to introduce robots to human environments such as hospitals, assembly lines, or houses, to help us in executing a large diversity of tasks. The key aspect of this is an efficient acquisition of new skills, where learning from the humans seems like one the most promising solutions. In this direction, a well-known learning from demonstration (LfD) framework is based on robot learning new skills from examples of tasks performed by humans.

LfD can be carried out through several approaches, each having its pros and cons. A very intuitive and inexpensive approach is kinaesthetic guidance where the human holds the robot limb and physically guides it to perform the desired task [1]–[3]. Some of the drawbacks of kinaesthetic teaching are: inability to teach the robot at a distance, undesirable dynamics induced by the human during the teaching and difficulty to simultaneously modulate other parameters, such as impedance [4]–[6]. An alternative is teaching through teleoperation where the human performs and teaches the task by controlling the robot through human-robot interfaces [5]–[8]. While in teaching through teleoperation we can avoid some of the drawbacks of kinaesthetic teaching, they usually require expensive hardware such as haptic devices, and involve to train the demonstrator to use them. Another alternative is learning from observation, where the human performs the task on his/her own, while the robot then learns from the observation.

In cases of complex tasks, the process of transforming the observation into a robotic skill may require an expert human involvement. The human may have to segment the data and analyse what variables are important to determine the appropriate task-frame control strategy. The most basic aspect of the task-frame control strategy is defining an appropriate controller for each axis based on what variable should have the priority (i.e. position, velocity, impedance, force). Hence, the controller for each axis can be determined manually by the human expert if the task is well-defined and if the expert human's involvement can be afforded [9], [10]. A more convenient alternative is to let the robot determine this autonomously based on the observation obtained from the human examples of the task.

A. Related Work

The automatic selection of controllers from human demonstrations of a task may be alternatively understood as the extraction of task constraints (which, in turn, may determine the type of the controller to be used). In this context, Mühlig *et al.* proposed an approach for the automatic selection of task spaces in the context of LfD [11]. A task space selector analyses the observed object trajectories and acquires task space descriptors that match the observation best. The selection mechanisms incorporate several criteria based on variance, psychological aspects and kinematics, to carry out the selection from a collection of different (and possible conflicting) task spaces. Despite the rich set of criteria used for the selection process, this work was solely applied to vision-tracked human demonstrations and tasks that did not consider the physical interaction with the environment where force controllers are crucial.

In [12], the analysis of task constraints in LfD was extended to the joint space of the robot. The proposed approach relied on

Manuscript received: September, 10, 2016; Revised December, 5, 2016; Accepted December, 31, 2016.

This paper was recommended for publication by Editor Dongheui Lee upon evaluation of the Associate Editor and Reviewers' comments.

Authors are with HRI^2 Lab and Learning and Interaction Lab, Department of Advanced Robotics, Istituto Italiano di Tecnologia, Via Morego 30, 16163 Genoa, Italy, Email: {luka.peternel; leonel.rozo; darwin.caldwell; arash.ajoudani}@iit.it

*Corresponding author.

Digital Object Identifier (DOI): see top of this page.

a probabilistic representation of the demonstrated data using Gaussian mixture models, which encapsulated the observed generalised velocities on both Cartesian and joint spaces. An optimal controller was found by using the product of normal distributions and inverse kinematics in order to combine the constraints of both spaces and generate desired joint velocities. The influence of the constraints was determined by the variability observed in the task spaces during the demonstrations. Similar to [11], the authors did not consider tasks where force control was needed, which limits the range of tasks in which the approach can be used. Moreover, the proposed approach exclusively depended on the data variability which assumes that the demonstrator will provide sufficient statistical information about the task.

A recent study [13] proposed a method that enabled the robot to autonomously determine the task constraints from the human-demonstrated data. The importance of each variable was high if it changed significantly within the single demonstration and if it changed systematically across multiple demonstrations. Based on this importance criterion, the robot then selected which variable (i.e. position or force) will be controlled in each axis of task frame. The main limitation of this method is that it overlooks the importance of variables that are to be kept at some constant level (i.e. constant force production in case of surface wiping [9], [14] or sawing [5], [10]), as the demonstrated data will not change significantly within the single demonstration and therefore not fit the significance criterion. In addition, if equivalent change of two variables is simultaneously observed, the method will treat them as equally significant. This may lead to a conflict and undesirable definition of controller for the observed task frame axis. One such example is when significant change in the force is merely a side effect of position production through some dynamics.

In a similar vein, repeated patterns and variability information observed in the human demonstrations have been used to learn position and force constraints in a human-robot collaboration scenario [15]. The approach uses a task-parametrised probabilistic model to automatically learn the task constraints. However, no specific distinction regarding the controller to be used at each task frame is provided. Therefore, this approach finds a trade-off between position and force control commands when a conflict between them exists.

B. Contributions

In this paper we propose an alternative method for the robot to autonomously derive the task-frame control strategy from the human-demonstrated data without knowing the demonstrated task objectives. We hypothesise that the importance of each observed variable should be determined by the following conditions:

1) if the observed pattern of a variable (i.e. position, force) in a single observation is consistent throughout multiple demonstrations, the variable should have a high importance and should be controlled in that axis,
2) if a considerable constant force offset (above some threshold) and some positional variability (below some threshold) are observed in the same axis simultaneously, it should be assumed the positional variability is an undesirable effect of force production,
3) if an equivalent importance is observed in two different variables in the same axis and if their patterns are correlated, it should be assumed that force pattern is a side effect of position generation, and therefore priority is given to the latter,
4) if no consistency in motion and force was observed and if the force offset is negligible (below some threshold), the axis should be set as a free (compliant) axis.

We implement the setup for collecting the human demonstrations through a motion capture system, a force sensor mounted on the tool and a human muscle activity measurement system. We use human muscle activity information to allow the robot to directly estimate an approximate stiffness behaviour for the given task. This approach differs from [13] in which the stiffness was determined indirectly through the relative importance between position and force variables in a certain axis. Note that the robot autonomous behaviour is driven by a hybrid force/impedance controller, which offers a good performance in cases when the task involves physical interaction with environment or a human [9], [10], [13].

To validate the proposed approach we conducted experiments using KUKA Lightweight Robot (LWR) and Pisa/IIT Softhand. We considered teaching the robot two tasks: surface wiping, material sawing and drilling. These experiments represent common daily-life tasks and involve coordinated motion and force production through physical interaction with the environment. Therefore, they provided an appropriate testbed for the proposed method.

The remainder of the paper is organised as follows: Section II describes the setup for collecting the demonstrations, introduces the control strategy derivation proposed in this paper, and presents the hybrid force/impedance robot controller. The surface wiping and material sawing experiments and corresponding results are reported in Section III. The pros and cons of the approach along with future work prospectives are discussed in Section IV.

II. Methods

The proposed method for the derivation of task-frame control authority from human examples was split into three main parts, namely: human demonstration, task definition and autonomous task execution by the robot. The purpose of human demonstration was to obtain the data about the task execution, which the robot can use as an observation. The demonstrator did not directly specify the task to the robot. Instead, the robot extracted the appropriate controllers through the proposed control strategy derivation method using the observed human examples of the task. The robot then used the defined control strategy and the extracted reference trajectories in the autonomous task execution.

A. Human Demonstration

The human demonstration was observed through a setup shown in Fig. 1. We measured the motion of human arm

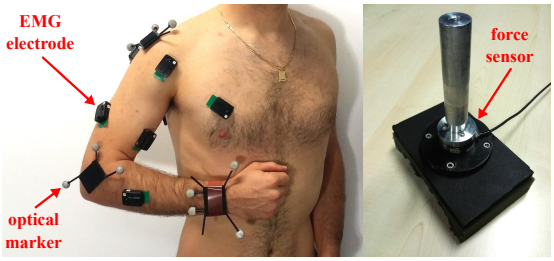

Fig. 1: Human demonstration setup. Motion capture system was used to measure the human arm kinematics (left photo). Tool was equipped with a force sensor to measure the interaction forces between the arm end-point and environment (right photo). Electromyography (EMG) was used to measure the human muscle activities in the arm.

during the task execution by an optical motion capture system (NaturalPoint OptiTrack) composed of 12 cameras working at a rate of 30 fps. The motion data was sampled at 100 Hz. We measured the forces at the human end-point by a force sensor mounted on the tool. We used muscle activity measurements to observe a general stiffness behaviour of the human arm during the task. All measurements were collected synchronously in real-time in the tool reference frame.

Human muscle activity was obtained through electromyography (EMG). The EMG data was sampled at 1000 Hz. For this purpose we used Delysis Trigno Wireless EMG system. The relation between human muscle activity and measured EMG signals was defined as

$$A_i(t) = \frac{EMG_i(t)}{MVC_i}, \tag{1}$$

where A_i is muscle activation level ($A \in [0, 1]$), EMG_i is EMG signal and MVC is EMG measured at maximal voluntary contraction of muscle i. We measured eight major muscles involved in the control of the arm: pectoralis major (PM), latissimus dorsi (LD), anterior deltoid (AD), posterior deltoid (PD), biceps brachii (BB), triceps brachii (TB), flexor carpi radialis (FC) and extensor carpi radialis (EC). In this study, we considered relatively large number of muscles related to the arm movement. In a more practical setup however, fewer muscles can be considered for a sufficient stiffness estimation [10], [16], as it is deemed that muscle activities among the muscles in human limbs follow synergetic patterns [17].

B. Task Defintion

The observed sensory data from the human demonstration was used by the robot to extract and define the task. The proposed task definition method consists of three sequential stages: data segmentation, task-frame control strategy derivation and impedance behaviour derivation.

1) Data Segmentation: In the first stage, the raw observed data was segmented into parts that could be used in the analysis. For example, in surface wiping task the agent has to produce a periodic motion along the surface plane, while producing the force perpendicularly to the surface so that friction can make the cleaning action. The robot should detect the periodical behaviour (if one exists) and treat it as a repetitive demonstration/observation of the same action. This can be carried out by methods such as the Adaptive Frequency Oscillator [18] or Dynamic Time Warping [19]. In this proof-of-concept study we did not focus on segmentation, therefore we segmented the data manually. We normalised each repeated observation of variable v to phase ϕ and calculated the phase-dependant mean (reference) trajectory $\boldsymbol{\mu}_v(\phi)$ and its standard deviation $\boldsymbol{\sigma}_v(\phi)$, which were used in the analysis in the next stage.

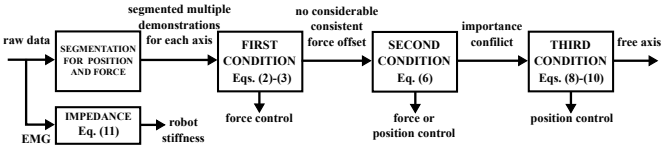

Fig. 2: Block scheme of controller-derivation algorithm for each axis. The algorithm collects human-demonstrated data and sequentially checks three main conditions in attempt to determine the control strategy for a given axis of the task frame. The *first condition* checks for repetitive force offsets. The *second condition* checks for repetitive patterns/trajectories of all variables. The *third condition* checks if force pattern is related to position pattern production when there is an importance conflict between the two variables. If none of the three conditions is met, the axis is set as free (i.e. impedance control with zero stiffness). The muscle activity measurements are used to determine the stiffness behaviour of the robot end-effector.

2) Task-Frame Control Strategy Derivation: In the second stage, after the raw data is segmented into repeated demonstration/observation of the same action, we examined the motion and force signals in each of the task frame axis to derive the control strategy. We checked the data consistency between repeated observations to extract the position/force behaviour. The proposed method followed the basic principles stated in Section I-B.

The method sequentially followed three main conditions (see Fig. 2), which incorporate the aforementioned principles. The control strategy derivation method started with the *first condition*, which checked if there was some considerable force offset observed consistently over multiple segmented observations in certain axis. In that case we prioritised the force offset control in that axis, even if there was some consistent position pattern in the same axis or some negligible force pattern around the offset. We assumed that slight position and force deviations can be most likely attributed to imperfect maintaining of the constant force during the practical human execution. To delegate the constant force regulation in a specific axis, the following criteria must be fulfilled in AND logical conjunction

$$f_1 = \frac{\left|\text{mean}\left(\boldsymbol{\mu}_F(\phi)\right)\right|}{\text{mean}\left(\boldsymbol{\sigma}_F(\phi)\right)} > f_{th1}, \tag{2}$$

$$f_2 = \frac{f_1}{\left|\max\left(\boldsymbol{\mu}_F(\phi)\right) - \min\left(\boldsymbol{\mu}_F(\phi)\right)\right|} > f_{th2}, \tag{3}$$

where f_1 is the force offset normalised to consistency (given by the observed mean standard deviation of the variable), f_{th1} is a force offset threshold, f_2 is the force offset normalised to amplitude (range) of the varying pattern around the offset and f_{th2} is a threshold ratio between the average force offset f_1 across the multiple observations and the amplitude of consistent pattern around that offset. The purpose of (3) is to check if the offset is dominant compared to the varying pattern around that offset. It prevents delegating force offset

control in case the pattern around the offset is more dominant than the offset itself.

If the *first condition* did not determine the axis controller for a constant force offset, the method proceeded to the *second condition* that checked for repetitive patterns/trajectories of all variables in a certain axis. We first observed the consistency of each variable across multiple observations. We defined an importance measure based on the consistency of repeated observations normalised by the amplitude (range) of mean trajectory across the action

$$c_v = \frac{\text{mean}\big(\boldsymbol{\sigma}_v(\phi)\big)}{\big|\max\big(\boldsymbol{\mu}_v(\phi)\big) - \min\big(\boldsymbol{\mu}_v(\phi)\big)\big|}, \tag{4}$$

$$w_v = \frac{1}{c_v}, \tag{5}$$

where c_v is variability estimation, w_v is the importance weight based on consistency, $\boldsymbol{\sigma}_v$ is a vector of standard deviation from the mean trajectory $\boldsymbol{\mu}_v$ across the phase ϕ of the segmented repeated observations of some variable v (i.e. position or force).

The *second condition* was based on comparing the consistency importance weights w_v between different variables v within the same axis. The controller for each axis was defined by the following criteria

$$\text{axis} = \begin{cases} \text{position} & \text{if } w_x > w_{th} \wedge w_F < w_{th} \\ \text{force} & \text{if } w_F > w_{th} \wedge w_x < w_{th}, \\ \text{conflict} & \text{if } w_x > w_{th} \wedge w_F > w_{th} \\ \text{free} & \text{if otherwise} \end{cases} \tag{6}$$

where w_x is position importance weight, w_F is force importance weight and w_{th} is a threshold value that determines whether the importance of the variable is significant or not. *Free axis* means compliant behaviour of the robot in that axis. In such case it can be potentially restricted by environmental constraints or controlled by a cooperating human [10].

If the *second condition* indicated a conflict between the importance of two variables in the same axis, the method proceeded to the *third condition*. To solve the conflict between position and force importance as given by the selection algorithm (6), we used a basic dynamics model as a criterion in the arbitration process. In cases of dynamical tasks, especially in tasks that involve interaction of environment, the motion and force relation can be modelled by the dynamics of a mass-spring-damper system

$$F = m\ddot{x} + b\dot{x} + kx, \tag{7}$$

where F and x are observed force and position, and m, b and k are dynamical parameters. The number and complexity of models that should be included and scanned through can be determined according to the general purpose of the robot and what kind of tasks it is expected to perform.

If the observed motion and force patterns with a similar importance were consistent with (7), the force pattern was assumed to be part of motion pattern generation. To check this relation, we calculated the derivatives of position and normalised them to their amplitude. The normalised derivatives were then compared to the normalised force pattern. To prefer the position over the force pattern, the following criteria must be fulfilled in OR logical conjunction

$$q_k = \text{mean}(|\boldsymbol{F}_* - \boldsymbol{x}_*|) < q_{th}, \tag{8}$$

$$q_b = \text{mean}(|\boldsymbol{F}_* - \dot{\boldsymbol{x}}_*|) < q_{th}, \tag{9}$$

$$q_m = \text{mean}(|\boldsymbol{F}_* - \ddot{\boldsymbol{x}}_*|) < q_{th}, \tag{10}$$

where subscript $*$ indicates that the variable is normalised to its amplitude, q_k, q_b and q_m are consistency measures for each part of the model (7) and q_{th} is the threshold that determines significance. If any of the measures was below q_{th}, the method assumed that the force pattern was related to the position pattern production.[1]

After the basic control strategy was defined for each axis, we used the mean values across the multiple repeated demonstrations to determine the reference value or trajectory $\boldsymbol{\mu}_v(\phi)$ for each variable v. If the extracted strategy determined the generation of some constant force offset in a certain axis (*first condition*), we used the mean of observed force offset as a reference for the force controller. If the extracted strategy prescribed following some position (*second or third condition*) or force pattern (*second condition*), we used Dynamical Movement Primitives (DMPs) [20] to encode the average observed position/force trajectory across the repeated demonstrations in a certain axis.

3) Impedance Behaviour Derivation: In the third (final) stage, we examined the observed human muscle activity data to see if some general stiffness behaviour could be extracted. Due to the spring-like properties of the human muscles [21], the muscle activation increases the stiffness of the individual muscle, which in turn increases the stiffness of the joint in the corresponding direction. Since mechanical structures of human and robot arm were different, we used the muscle activity only as a general trend indicator for the robot stiffness behaviour.

The proposed stiffness behaviour extraction method compared the amplitude of the previously selected control variables in each axis to the amplitude of the observed human muscle activity between different trials (if they existed). Here it is assumed that a different trial exhibits some variation of the task performance (e.g., wiping the surface more intensely when stains are more resistant, etc.). The condition determining the importance of stiffness behaviour with respect to the behaviour of each variable was defined as

$$s_v = \frac{\frac{\text{mean}(\boldsymbol{\mu}_v^i)}{\text{mean}(\boldsymbol{A}^i)}}{\frac{\text{mean}(\boldsymbol{\mu}_v^j)}{\text{mean}(\boldsymbol{A}^j)}} \in \left[\frac{1}{s_{th}}, s_{th}\right], \tag{11}$$

where s_v is the importance factor for the stiffness behaviour, s_{th} is ratio threshold that determines the importance and $\boldsymbol{A}$ is a vector containing the mean values of observed reference activity for each muscle across the segmented action. Superscripts in each variable represent different human demonstration trail. If factor s_v is close to one, it hints that there is a consistent relation between amplitude change of human muscle activity

[1]The criterion could also mean that position is related to force production. Due to the impedance-admittance duality, controlling either force or position should produce the observed patterns. Therefore, we decided to prefer position since its control/measurement is generally easier.

(which is related to stiffness) and change of the amplitude of the observed variable.

If a significant correlation was detected, the robot Cartesian stiffness matrix was a function of variable v

$$\boldsymbol{K} = \boldsymbol{K}_{const} + \boldsymbol{K}_{ctrl}(v), \tag{12}$$

where $\boldsymbol{K}$ is Cartesian stiffness matrix and $\boldsymbol{K}_{ctrl}(v)$ is stiffness behaviour dependant on the variable v. Matrix $\boldsymbol{K}_{const}$ is used to keep some constant minimum stiffness in order to ensure the position tasks are always tracked. If no significant correlation was detected, the axes with position controller used the constant minimum stiffness defined in $\boldsymbol{K}_{const}$.

C. Autonomous Robot Controller

After the definition of the task-frame control strategy based on the observed demonstration data, the strategy was used by the robot in the autonomous operation. The robot task frame behaviour was governed by a hybrid force/impedance controller defined as

$$\boldsymbol{F}_{int} = \boldsymbol{F}_{imp} + \boldsymbol{F}_{for}, \tag{13}$$

where $\boldsymbol{F}_{int}$ is a task frame end-effector force acting from the environment on the robot, $\boldsymbol{F}_{imp}$ is end-effector force related to the position-control tasks (through impedance control) and $\boldsymbol{F}_{for}$ is end-effector force related to force-control tasks. The force was controlled by PI controller.

The position-control tasks were controlled by an impedance controller

$$\boldsymbol{F}_{imp} = \boldsymbol{K}\big(\boldsymbol{x}_a - \boldsymbol{x}_d\big) + \boldsymbol{D}\big(\dot{\boldsymbol{x}}_a - \dot{\boldsymbol{x}}_d\big), \tag{14}$$

where $\boldsymbol{x}_a$ and $\boldsymbol{x}_d$ are actual and desired end-effector positions, $\boldsymbol{K}$ is Cartesian stiffness obtained by (12) and $\boldsymbol{D}$ is Cartesian damping matrix, which was obtained by *double diagonalisation design* [22].

III. Experiments

To validate the proposed method, we performed two experiments involving physical interaction with the environment: surface wiping with a sponge, material cutting with a saw and drilling. We used the setup described in Section II-A to collect the human demonstration data for each task. The robot then analysed and used the observed data to derive the task-frame control strategy without prior information about what kind of task was demonstrated to it. The obtained control strategy was later used to execute the desired task with a KUKA LWR manipulator. The reproduction setups for all tasks are shown in Fig. 3. The procedure and results for each task are presented in the respective subsections below. Please refer to supplementary multimedia file for the video of these experiments.

The parameters of the method were determined and selected experimentally based on the preliminary analysis. The parameters related to the *first condition* were set to $f_{th1} = 2$ and $f_{th2} = 0.1$, while those related to the *second condition* and *third condition* were set to $w_{th} = 5$ and $q_{th} = 0.3$, respectively. The parameter related to impedance behaviour derivation was set to $s_{th} = 2$.

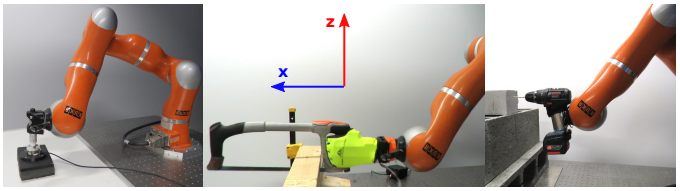

Fig. 3: Experimental setups for surface wiping (left), sawing (middle) and drilling (right). The observation frame was in all cases the same.

A. Surface Wiping

1) Learning Stage: The task of the human in this experiment was to demonstrate how to perform the surface wiping task. In the demonstration, we used a sponge with a force sensor mounted on it (see Fig. 1) to wipe a surface of a white board. The common strategy to perform this kind of task is to apply some force perpendicularly to the surface, while at the same time moving the sponge across the surface plane. The idea is to form a friction between the surface and the sponge that makes the cleaning action possible. While this strategy was known by the human, the robot did not have the information about the task and had to use the proposed method to extract the control strategy from the observed human data.

The results of the human demonstrations are shown in Fig. 4a. By observing the position (top row) we can see that the human made a repetitive elliptical motion on the plane of the surface (x-y) to perform the wiping action. Note that a lower force trial was conducted first, followed by a higher force trial (as shown in the middle plot). We can see that the human muscle activity increased when the force applied on the surface was higher.

The results of data analysis using the method described in Section II-B are shown in Fig. 4b. The z-axis passed the *first condition* ($f_1 > 2$ and $f_2 > 0.1$) and the method consequently prescribed control of force offset. In contrast, x and y axes did not pass the *first condition* and therefore the method proceeded to the *second condition* in order to check for consistent position and force trajectories. In both axes, the method detected a conflict in importance between position and force ($w_x > 5$ and $w_F > 5$), therefore the method continued to the *third condition* for the arbitration process. Since the second derivative of position was dynamically related to the sensed force through the mass part of (7), the *third condition* was satisfied ($q_m < 0.3$) and position control strategy was determined for both x and y.

Also note that a correlation between the increase of amplitude of force in z-axis and the increase of amplitude of muscle activity was observed ($s = 1.44 \in \left[\frac{1}{s_{th}}, s_{th}\right]$), the robot adopted the stiffness strategy described by (12). For stiffness behaviour, we assumed a linear relation model[2] between $\boldsymbol{K}_{ctrl}$ and the force along z, namely F_z

$$\boldsymbol{K}_{ctrl}(\boldsymbol{F}_z) = \boldsymbol{k}_K \cdot \boldsymbol{F}_z, \tag{15}$$

where $\boldsymbol{k}_K$ was set experimentally to 40 m^{-1} for x and y-axis and zero for z. $\boldsymbol{K}_{const}$ was set to 400 N/m for translational axes and 200 Nm/rad for rotational axes. Note that while

[2]Alternatively, more complex models can be used if more complex behaviour is required or extracted.

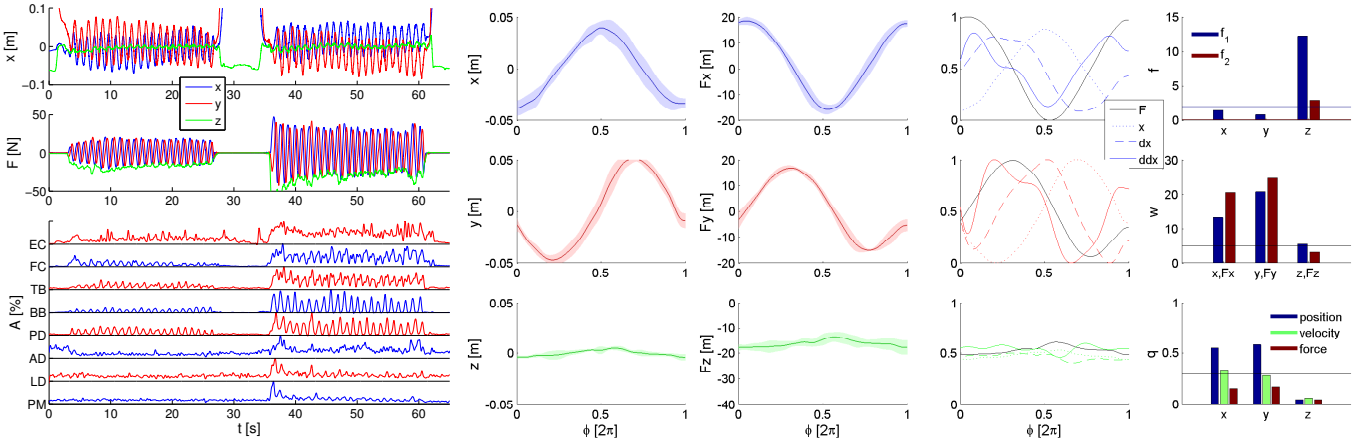

(a) Sensory observation (b) Analysis

Fig. 4: Results of control strategy derivation process for wiping task. The human demonstration is shown on the left side, and includes position, force and muscle activity data. The analysis related to conditions described in Fig. 2 is shown on the right side. The first column graphs are related to the segmented data for position, where solid line represents the mean trajectory and shaded area depicts the standard deviation. The second column graphs show the same for the force. The third column graphs are related to comparison to mass-spring-damper dynamics (7), where dotted line is the normalised position, dashed line is the normalised velocity, solid line is the normalised acceleration and black solid line is the normalised force trajectory. The fourth column shows different weights used in the task-frame control strategy derivation. The top graph shows the weights for determining force offset (blue bar is f_1 and red bar is f_2). The middle graph shows the weight for position (blue bar) and force (red bar). The bottom graph shows the weight used in comparison to mass-spring-damper dynamics (blue bar is related to spring, green bar to damper and red bar to mass). Thresholds are indicated by horizontal lines.

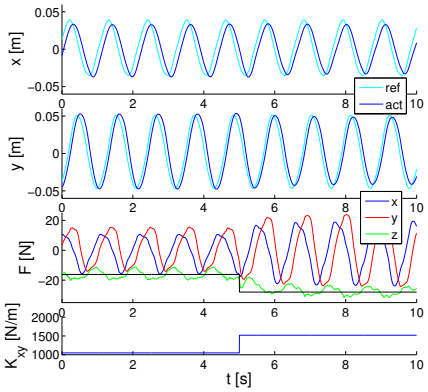

Fig. 5: Results of autonomous robot surface wiping experiment. The first graph shows reference and actual motion in x-axis. The second graph shows the same for y-axis. The third graph shows the force sensor measurements (black line corresponds to z-axis reference force). The fourth graph shows the robot end-effector stiffness in x and y-axis.)

changes in axis with force control correlate with changes in muscle activity and consequently stiffness, only axes with position control can be affected by the changing stiffness (impedance). Changing stiffness naturally does not affect the force controller.

2) Autonomous Stage: When the robot extracted the control strategy from the observed human data, we carried out the autonomous reproduction of surface wiping experiment. To show some degree of robustness of devised strategy we used it to perform surface wiping on two different surfaces: whiteboard (smooth surface) and concrete (rough surface). Please refer to supplementary multimedia file for the video of the experiment.

The results of this experiment are shown in Fig. 5. Observe that the first and the second graphs show that the robot followed the desired elliptical position reference trajectory on the surface parallel to the x-y plane. As we can see from the third graph, the robot simultaneously produced the desired constant force in z-axis, perpendicularly to the surface generated the required friction for the wiping. The force reference was changed during the experiment between the two references that were extracted from the two different demonstration trials (i.e. 16.2 N and 28.0 N). While this change occurred, the robot also adjusted the stiffness in x-axis and y-axis in accordance to the extracted stiffness behaviour from the demonstration data. This change is shown in the fourth graph.

B. Material Sawing

The goal of this experiment was to demonstrate to a robot how to perform a sawing task to cut a material from human examples. In the demonstration stage, we used a saw that had a force sensor mounted on it to perform the sawing action. During the sawing, the saw blade had to be periodically moved from one side of the blade to the other in a straight line across the intended incision location. At the same time, some force had to be applied toward the cutting direction to keep the contact and produce the sufficient friction for the cutting. The demonstrator was instructed to perform two trials, each with different cutting force. The demonstrator also showed how to perform sawing at different locations along the y-axis (along the beam).

The results of human demonstration are shown in Fig. 6a. By observing the position trajectories (first graph) we can see that the human made a repetitive motion in sawing axis (x-axis) to drive the blade. As in the previous experiment, the lower force trial was conducted first and the higher force trial was conducted later (see second graph).

The results of data analysis using the method described in Section II-B are shown in Fig. 6b. The z-axis passed the *first condition* ($f_1 > 2$ and $f_2 > 0.1$) and the method prescribed control of force offset. The x and y axes did not pass the *first condition* and therefore the method proceeded to the

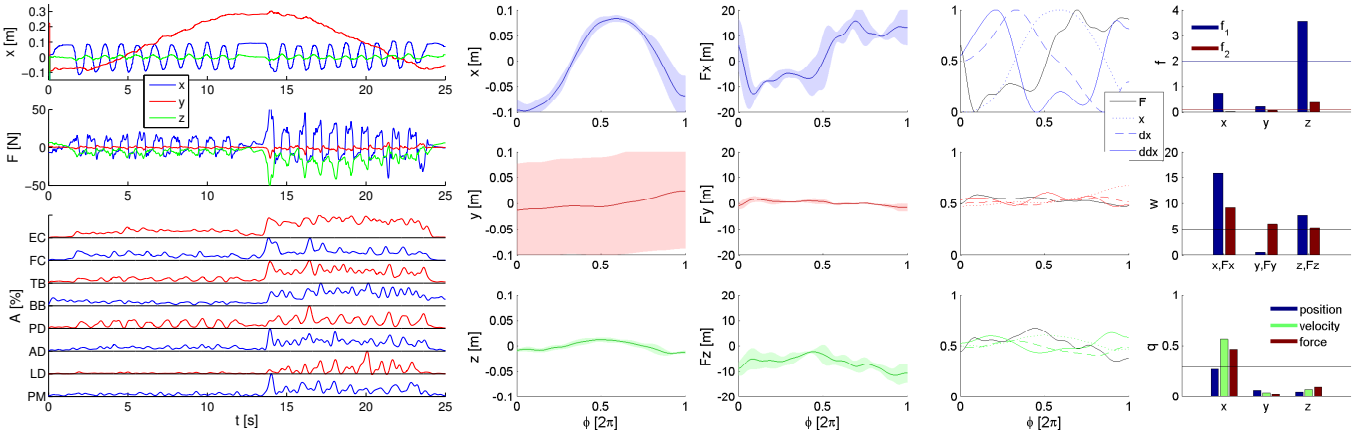

(a) Sensory observation (b) Analysis

Fig. 6: Results of control strategy derivation process for sawing task. The graphs display the same parameters as those in Fig. 4b. The human demonstration is shown on the left side, and includes position, force and muscle activity data. The analysis related to conditions described in Fig. 2 is shown on the right side.

second condition to check for consistent position and force trajectories. The algorithm detected a conflict in importance between position and force in the x axis ($w_x > 5$ and $w_F > 5$) and therefore the method continued to the *third condition* for arbitration process. Since the position was related to the force through spring part of (7), the *third condition* was satisfied ($q_k < 0.3$) and position control strategy was determined for x-axis.

Note that since the human demonstrated the sawing task at various locations along y-axis, the consistency in position across the multiple segmented observations in that axis was low and well below the threshold $w_x < 5$. In contrast to the wiping experiment, here the detected force consistency in y-axis was relatively high and showed a value just above the threshold $w_F > 5$, therefore the force controller was prescribed for this axis. It is worth highlighting that the mean force in y is almost zero through the phase (see bottom graph in second column of Fig. 6b). Zero-force control can be beneficial in keeping the saw from bending in y-axis, which is undesirable in this task. In contrast to position control, zero-force control is position independent and can therefore be more robust to perturbations, such as displacement of wood position in y-axis.

We observed a correlation between the amplitude of force in cutting direction (z-axis) and the amplitude of muscle activity ($s = 0.90 \in \left[\frac{1}{s_{th}}, s_{th}\right]$). So, we used (15) to describe the relation between robot stiffness and force, where $\boldsymbol{k}_K$ was set experimentally to 40 m^{-1} for x-axis and zeros for the rest of the axes. The minimum constant stiffness was set to 400 N/m, same as in the previous task.

For demonstration of autonomous robot sawing task execution using the devised strategy please refer to supplementary multimedia file. To show the robustness of the devised strategy we used it to perform the task on two different materials: wood and brick.

C. Drilling

In this experiment the task of the human was to demonstrate how to perform the drilling task. To use a drilling machine, the force perpendicular to the surface has to be increased and kept at some level to gradually move the drill inside the material. When the drilling is to be stopped, the force must be reduced to halt the operation. The main difference between this task and the previous two tasks is that this one can be considered non-periodic.

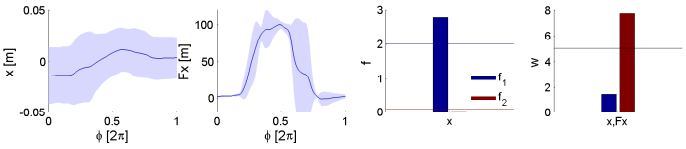

Fig. 7: Results of control strategy derivation process for drilling task. The graphs display the same parameters as those in Fig. 4b.

Results of the learning experiment are shown in Fig. 7, where we focus on the drilling direction axis (x-axis) that is important in this task. While the observed force offset was large ($f_1 > 2$), the consistent pattern around the offset was more dominant ($f_1 < 0.1$), therefore the *first condition* did not pass. In the *second condition*, the proposed method derived force control in this axis because a consistent force profile was detected across repeated demonstrations ($w_F > 5$). Since the drill moved gradually inside the material after each repeated demonstration, the position variation in the drilling axis was large ($w_x < 5$) and therefore the force production task was preferred over the position control.

After we derived the appropriate robot skill for this task execution, we used it to make the robot perform the task autonomously. For demonstration of autonomous execution please refer to multimedia file.

IV. Discussion

The proposed method enables the robot to derive the task-frame control strategy from the observed human demonstrations without any prior knowledge of the demonstrated task. The strategy is carried out by analysing different criteria built on the variability of the demonstrations, their value range, magnitude, observed patterns, and the dynamics of linear systems. In such a way, the robot is able to determine whether

a control action is required at each task axis (and the type of controller to be used) or it should behave compliantly otherwise. Therefore, this method augments the robot's autonomy and reduces the amount of human intervention in the learning process.

The method requires the repeated demonstrations of the same task, which might make it intrinsically more suitable for periodic tasks. However, the method is not limited to periodic tasks, as long as repeated demonstrations of the same task can be provided.

A possible limitation of observing the human demonstration to extract robotic skills is that these are optimised for humans and might not be completely optimal for the robot. In addition, the method relies on several important parameters, where the most crucial are: f_{th1}, f_{th2} and w_{th}. In this direction, optimisation methods or reinforcement learning can be used in conjunction with our method so that the robot can refine the parameters or the obtained control strategy by itself. Another potential disadvantage is related to the human demonstration setup, where external sensory systems (motion capture system, tools with force sensor and EMG) are required during the observation stage. As an alternative, kinaesthetic teaching may be used instead to make the human demonstration, and afterwards the proposed method can extract the control strategy.

If more complex behaviour is observed in the same axis, e.g. some portion of period requires force control while the other position control, more complex segmentation could be employed in order to derive different control strategy in different sections of the main observation period.

The performance of the autonomous task execution mainly depends on how well the human performed the task during demonstration. Some quantitative measures could be defined to evaluate the performance of the task. However, such measures would primarily evaluate the human task performance during the demonstration, provided that the correct control strategy is derived and the robot imitates the human demonstrations well.

The increased impedance due to the increased muscle activity was biologically motivated and human-like [21]. Possible advantages of increasing stiffness due to the increased muscle activity are related to task performance and robustness. For example, when interaction force is increased, the increased friction may affect the position tracking (e.g., wiping task). Increased stiffness in this case makes the position tracking more accurate according to the impedance control law (14). In another example, production of higher forces in unpredictable environment is inherently more dangerous when exposed to external perturbations. Increased stiffness in this case provides more stabilisation to the arm and may offer more robust operational conditions.

In future we will put more stress into the analysis of muscle activity, where we plan to exploit probabilistic machine learning techniques to discover complex relations between the muscle contractions and the movements and forces generated at the task axes. Additionally, more sophisticated models will be considered for representing the stiffness-force relation.

REFERENCES

[1] M. Hersch, F. Guenter, S. Calinon, and A. Billard, "Dynamical system modulation for robot learning via kinesthetic demonstrations," *IEEE Trans. on Robotics*, vol. 24, no. 6, pp. 1463–1467, 2008.

[2] D. Lee and C. Ott, "Incremental kinesthetic teaching of motion primitives using the motion refinement tube," *Autonomous Robots*, vol. 31, no. 2, pp. 115–131, 2011.

[3] L. Rozo, S. Calinon, D. G. Caldwell, P. Jimnez, and C. Torras, "Learning physical collaborative robot behaviors from human demonstrations," *IEEE Trans. on Robotics*, vol. 32, no. 3, pp. 513–527, June 2016.

[4] A. Ajoudani, *Transferring Human Impedance Regulation Skills to Robots*. Springer, 2016.

[5] L. Peternel, T. Petrič, E. Oztop, and J. Babič, "Teaching robots to cooperate with humans in dynamic manipulation tasks based on multi-modal human-in-the-loop approach," *Autonomous robots*, vol. 36, no. 1-2, pp. 123–136, Jan 2014.

[6] L. Peternel, T. Petrič, and J. Babič, "Human-in-the-loop approach for teaching robot assembly tasks using impedance control interface," in *IEEE Intl. Conf. on Robotics and Automation (ICRA)*, May 2015, pp. 1497–1502.

[7] P. Evrard, E. Gribovskaya, S. Calinon, A. Billard, and A. Kheddar, "Teaching physical collaborative tasks: object-lifting case study with a humanoid," in *IEEE-RAS Intl. Conf. on Humanoid Robots*, 2009, pp. 399–404.

[8] P. Kormushev, S. Calinon, and D. G. Caldwell, "Imitation Learning of Positional and Force Skills Demonstrated via Kinesthetic Teaching and Haptic Input," *Advanced Robotics*, vol. 25, no. 5, pp. 581–603, 2011.

[9] C. Schindlbeck and S. Haddadin, "Unified passivity-based cartesian force/impedance control for rigid and flexible joint robots via task-energy tanks," in *IEEE Intl. Conf. on Robotics and Automation (ICRA)*, May 2015, pp. 440–447.

[10] L. Peternel, N. Tsagarakis, and A. Ajoudani, "Towards multi-modal intention interfaces for human-robot co-manipulation," in *IEEE/RSJ Intl. Conf. on Intelligent Robots and Systems (IROS)*, October 2016, pp. 2663–2669.

[11] M. Mühlig, M. Gienger, J. J. Steil, and C. Goerick, "Automatic selection of task spaces for imitation learning," in *IEEE Intl. Conf. on Intelligent Robots and Systems (IROS)*, October 2009, pp. 4996–5002.

[12] S. Calinon and A. Billard, "Statistical learning by imitation of competing constraints in joint space and task space," *RSJ Advanced Robotics*, vol. 23, pp. 2059–2076, 2009.

[13] A. Ureche, K. Umezawa, Y. Nakamura, and A. Billard, "Task parameterization using continuous constraints extracted from human demonstrations," *IEEE Trans. on Robotics*, vol. 31, no. 6, pp. 1458–1471, Dec 2015.

[14] A. Gams, T. Petrič, M. Do, B. Nemec, J. Morimoto, T. Asfour, and A. Ude, "Adaptation and coaching of periodic motion primitives through physical and visual interaction," *Robotics and Autonomous Systems*, vol. 75, Part B, pp. 340 – 351, 2016.

[15] L. Rozo, D. Bruno, S. Calinon, and D. G. Caldwell, "Learning optimal controllers in human-robot cooperative transportation tasks with position and force constraints," in *IEEE/RSJ Intl. Conf. on Intelligent Robots and Systems (IROS)*, 2015.

[16] A. Ajoudani, C. Fang, N. G. Tsagarakis, and A. Bicchi, "A reduced-complexity description of arm endpoint stiffness with applications to teleimpedance control," in *IEEE/RSJ Intl. Conf. on Intelligent Robots and Systems (IROS)*, Sept 2015, pp. 1017–1023.

[17] M. Turvey, "Action and perception at the level of synergies," *Human Movement Science*, vol. 26, no. 4, pp. 657–697, 2007.

[18] T. Petrič, A. Gams, A. J. Ijspeert, and L. Žlajpah, "On-line frequency adaptation and movement imitation for rhythmic robotic tasks," *Intl. Journal of Robotics Research*, vol. 30, no. 14, pp. 1775–1788, Dec. 2011.

[19] L. Wang, W. Hu, and T. Tan, "Recent developments in human motion analysis," *Pattern Recognition*, vol. 36, no. 3, pp. 585 – 601, 2003.

[20] A. J. Ijspeert, J. Nakanishi, and S. Schaal, "Learning rhythmic movements by demonstration using nonlinear oscillators," in *Intelligent Robots and Systems (IROS), 2002 IEEE/RSJ Intl. Conf. on*, 2002, pp. 958–963.

[21] F. A. Mussa-Ivaldi, N. Hogan, and E. Bizzi, "Neural, mechanical, and geometric factors subserving arm posture in humans," *The Journal of Neuroscience*, vol. 5, no. 10, pp. 2732–2743, Oct. 1985.

[22] A. Albu-Schäffer, C. Ott, U. Frese, and G. Hirzinger, "Cartesian impedance control of redundant robots: recent results with the DLR-light-weight-arms," in *IEEE Intl. Conf. on Robotics and Automation (ICRA)*, vol. 3, Sept 2003, pp. 3704–3709.